# Fast Localized Voltage Regulation in Single-Phase Distribution Grids

Vassilis Kekatos,[1] Liang Zhang,[1] Georgios B. Giannakis,[1] and Ross Baldick[2]
[1]Digital Tech. Center and Dept. of ECE, Univ. of Minnesota, Minneapolis, MN 55455, USA
[2]ECE Dept., University of Texas at Austin, TX 78712, USA
{kekatos,zhan3523,georgios}@umn.edu, baldick@ece.utexas.edu

***Abstract*—Distribution grids undergo a transformative change with the emergence of renewables, demand-response programs, and electric vehicles. Fluctuations in active power injections can dramatically affect voltage magnitudes across the grid. The power electronics of distributed generation (DG) units can provide an effective means of the much needed voltage regulation. On the other hand, the scalability and time-variability of DGs call for localized and fast-responding control schemes. In this context, a reactive power control rule recommended by the IEEE 1547 standard is interpreted here as a proximal gradient algorithm. Upon understanding its convergence rate limitations, an accelerated voltage regulation scheme is developed. The latter not only affords localized processing, but it further enjoys a notable speedup advantage with only a slight modification of the original control rule. Numerical tests on the IEEE 13-bus and 34-bus systems with high solar penetration corroborate its superior convergence rates.**

## I. Introduction

Environmental challenges together with the potential energy crisis have been transforming power distribution grids. On top of the conventional smooth consumer demand, distribution grids should nowadays accommodate renewables, elastic loads, and electric vehicles. Different from transmission grids, where bus voltage magnitudes are relatively invariant to active power injections, renewable generation and demand-response programs can give rise to major voltage fluctuations in medium- and low-voltage grids [22]. Rather than relying on slow-responding utility-owned voltage regulators and shunt capacitors, the advanced power electronics found in photovoltaics (PV), batteries, and electric vehicles, coupled with proper control algorithms, are capable of providing an effective means of auxiliary services such as voltage regulation.

Reactive power control leveraging distributed generation (DG) units has been an active area of research. Voltage regulation policies relying on linearized models are proposed in [22], while a successive convex approximation is adopted in [7]; see also [2] for a multi-agent technique. In [6], power loss minimization is effected using a decentralized consensus-type algorithm. The aforementioned schemes depend on approximate grid models and entail algorithms requiring fast two-way communication between adjacent buses.

If further resources are provided, a grid operator can employ DGs for power loss minimization while satisfying voltage regulation constraints. Reactive power management can then be solved centrally using a full AC grid model after collecting all nodal generations and demands; see e.g., [8], [15]. Considering the scale of DGs, decentralized algorithms based on the alternating-direction method of multipliers are also well motivated [21], [19], [5]. By exploiting the tree structure of distribution grids, these schemes require communication only between neighboring buses.

Nevertheless, real-time communication may be unrealistic in current distribution grids. For example, although 8,544 MW of solar energy has been installed in California, real-time communication between buses is rare [1]. Hence, local algorithms without communication requirements are needed. In this context, [20] advocates reactive power injections adjusted proportionally to the local voltage violations. Assuming unlimited reactive power resources, sufficient conditions guaranteeing convergence of the latter scheme are developed in [24]. Under a linearized power flow model and for constrained reactive power resources, a similar local control rule has been shown to minimize a modified voltage regulation cost [9]. A droop control strategy that adjusts the inverter voltage output by measuring the reactive power flow is proposed in [11].

In this work, the linear distribution flow model is postulated to derive localized voltage regulation schemes for single-phase grids. With an emphasis on the speed at which DG units solve this grid-wide resource allocation problem, our contribution is two-fold. First, a control rule advocated by the IEEE 1547 standard and reverse engineered in [9], is interpreted here as a proximal gradient algorithm. By doing so, its convergence and, perhaps more importantly, its convergence rate properties are fully characterized. Second, realizing that the convergence rate of this control rule depends on the grid topology, we propose an accelerated proximal gradient scheme. We further show that the novel scheme involves a minor modification in the control rule and it can still be implemented locally. Numerical tests on the IEEE 13-bus and 34-bus distribution grid benchmarks verify that the novel voltage regulation scheme offers a significant speedup advantage over its conventional alternative.

*Notation.* Lower- (upper-) case boldface letters denote column vectors (matrices), with the exception of line power flow vectors $(\mathbf{P}, \mathbf{Q})$. Calligraphic symbols are reserved for sets. Symbol $^\top$ stands for vector and matrix transposition. Vectors $\mathbf{0}$, $\mathbf{1}$, and $\mathbf{e}_n$, are the all-zeros, all-ones, and the $n$-th canonical vectors, respectively; while $\|\mathbf{x}\|_2$ denotes the $\ell_2$-

Work in this paper was supported by the Inst. of Renewable Energy and the Environment (IREE) under grant no. RL-0010-13, University of Minnesota, and NSF Grants 142331 and 1442686.

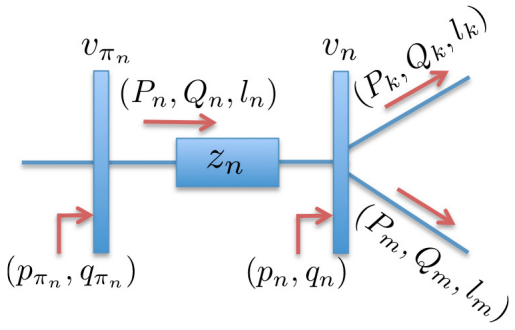


Fig. 1. Bus $n$ is connected to its unique parent $\pi_n$ via line $n$.

norm of vector $\mathbf{x}$. Symbol $\lambda_i(\mathbf{X})$ stands for the $i$-th largest eigenvalue; $\mathrm{diag}(\mathbf{x})$ defines a diagonal matrix having vector $\mathbf{x}$ on its diagonal, whereas $\mathrm{diag}(\mathbf{X})$ is the vector formed by the main diagonal of $\mathbf{X}$. Operators $\mathrm{Re}(z)$ and $\mathrm{Im}(z)$ return the real and imaginary part of complex number $z$. A matrix with non-negative entries is denoted by $\mathbf{X} \geq \mathbf{0}$, while a symmetric positive semi-definite matrix is indicated by $\mathbf{X} \succeq \mathbf{0}$.

## II. Radial Distribution Grid Modeling

Consider a radial single-phase distribution grid consisting of $N+1$ buses. Such a grid can be modeled by a tree graph $\mathcal{T} = (\mathcal{N}_o, \mathcal{L})$ whose nodes $\mathcal{N}_o := \{0, \ldots, N\}$ correspond to buses, and whose edges $\mathcal{L}$ to distribution lines with cardinality $|\mathcal{L}| = N$. The tree is rooted at the substation bus indexed by $n = 0$. For every bus $n \in \mathcal{N}_o$, let $v_n$ be its squared voltage magnitude and $s_n = p_n + jq_n$ its complex power injection. Every non-root bus $n \in \mathcal{N} := \{1, \ldots, N\}$ has a unique parent bus denoted by $\pi_n$; see Figure 1. Hence, the directed edge $(\pi_n, n) \in \mathcal{L}$ corresponding to the line feeding bus $n$ will be simply indexed by $n$. Without loss of generality, nodes can be numbered such that $\pi_n < n$ for all $n \in \mathcal{N}$, e.g., by a simple depth-first traversing of the tree. For every bus $n$, we further define the augmented set $\mathcal{D}_n$ including bus $n$ and its descendant buses.

The grid is modeled by the branch flow equations [3]

$$s_n = \sum_{k \in \mathcal{C}_n} S_k - S_n + \ell_n z_n \tag{1}$$

$$v_n = v_{\pi_n} - 2\,\mathrm{Re}[z_n^\star S_n] + \ell_n |z_n|^2 \tag{2}$$

$$|S_n|^2 = v_{\pi_n} \ell_n \tag{3}$$

where $z_n = r_n + jx_n$ is the impedance of line $n$; $\ell_n$ is the squared current magnitude on line $n$; $S_n = P_n + jQ_n$ is the complex power flow on line $n$ seen at the sending end; and $\mathcal{C}_n := \{k \in \mathcal{N} : \pi_k = n\}$ is the set of children nodes for bus $n$. Equation (1) follows from power conservation; (2) is derived upon squaring the second Kirchoff's law; and (3) is the definition of power flow. The branch flow model is essentially derived from the full AC model, after ignoring voltage and current phases. For the feeder, power injection satisfies $s_0 = \sum_{k \in \mathcal{C}_0} S_k$, and its voltage is fixed at the nominal level $v_0$.

The aforementioned model involves two linear equalities (1)-(2), and the quadratic equality (3) that complicates calculations. For everyday grid operations, an approximate model is oftentimes used instead. The so termed *LinDistFlow* model ignores (3), and because $\{r_n, x_n\}_{n \in \mathcal{L}}$ have relatively small entries, it drops the third summands in the right-hand sides of (1) and (2), yielding the approximate linear model [3]

$$s_n = \sum_{k \in \mathcal{C}_n} S_k - S_n \tag{4}$$

$$v_n = v_{\pi_n} - 2\,\mathrm{Re}[z_n^\star S_n]. \tag{5}$$

In the voltage regulation setup, active power injections $\{p_n\}_{n=1}^N$ are assumed known. The goal is to control reactive power injections $\{q_n\}_{n=1}^N$ so that squared voltage magnitudes $v_n$ are kept close to their nominal value $v_0$. Conventionally, injections $\{(p_n, q_n)\}$ represent non-controllable loads with the exception of a few buses with shunt capacitors whose $q_n$ can be adjusted at a slow pace. In the distribution grid setup, the $p_n$'s from DGs may fluctuate significantly, yet the associated PV inverters have digitally controllable $q_n$'s.

To characterize the behavior of voltage regulation schemes, the branch-bus incidence matrix $\tilde{\mathbf{A}} \in \mathbb{R}^{L \times (N+1)}$ is studied next. Matrix $\tilde{\mathbf{A}}$ defines the connectivity of the grid, since its entries are $\tilde{\mathbf{A}}_{n,\pi_n+1} = 1$ and $\tilde{\mathbf{A}}_{n,n+1} = -1$ for all $n \in \mathcal{N}$, and zero otherwise [12]. Partition $\tilde{\mathbf{A}}$ into the first and the rest of its columns as

$$\tilde{\mathbf{A}} := [\mathbf{a}_0 \ \mathbf{A}].$$

For a radial grid, the *reduced branch-bus incidence matrix* $\mathbf{A}$ is square and invertible. Matrix $\mathbf{A}$ and its negative inverse $\mathbf{F} := -\mathbf{A}^{-1}$ enjoy the following properties shown in the Appendix.

**Proposition 1.** *The reduced branch-bus incidence matrix* $\mathbf{A}$ *of a radial grid and its negative inverse* $\mathbf{F} := -\mathbf{A}^{-1}$ *satisfy:*
*(a)* $-\mathbf{A}^{-1}\mathbf{a}_0 = \mathbf{1}_N$*;*
*(b)* $\mathbf{A}$ *and* $\mathbf{F}$ *are lower triangular;*
*(c)* $-\mathbf{A}$ *and* $\mathbf{F}$ *have eigenvalues equal to one;*
*(d)* $-\mathbf{A}$ *is an M-matrix and thus* $\mathbf{F} \geq \mathbf{0}$*; and*
*(e) the entries of* $\mathbf{F}$ *are* $\mathbf{F}_{m,n} = 1$ *for* $n \in \mathcal{N}$ *and* $m \in \mathcal{D}_n$*; and zero, otherwise.*

Collect all nodal quantities related to non-root buses in vectors $\mathbf{p}$, $\mathbf{q}$, and $\mathbf{v}$; and all line quantities in vectors $\mathbf{r}$, $\mathbf{x}$, $\mathbf{P}$, and $\mathbf{Q}$. Their associated complex quantities are denoted by $\mathbf{s} := \mathbf{p} + j\mathbf{q}$, $\mathbf{z} := \mathbf{r} + j\mathbf{x}$, and $\mathbf{S} := \mathbf{P} + j\mathbf{Q}$. Having defined $\mathbf{A}$, the model in (4)-(5) can be compactly expressed as

$$\mathbf{s} = \mathbf{A}^\top \mathbf{S} \tag{6}$$

$$\mathbf{A}\mathbf{v} = 2\,\mathrm{Re}[\mathbf{Z}^\star \mathbf{S}] - \mathbf{a}_0 v_0 \tag{7}$$

where $\mathbf{Z} := \mathrm{diag}(\mathbf{z})$. Premultiplying (7) by $\mathbf{A}^{-1}$, substituting $\mathbf{S} = \mathbf{A}^{-\top}\mathbf{s} = -\mathbf{F}^\top \mathbf{s}$ from (6), and using the property $\mathbf{A}^{-1}\mathbf{a}_0 = -\mathbf{1}_N$, we obtain

$$\mathbf{v} = \mathbf{R}\mathbf{p} + \mathbf{X}\mathbf{q} + v_0 \mathbf{1}_N \tag{8}$$

where $\mathbf{R} := 2\mathbf{F}\,\mathrm{diag}(\mathbf{r})\mathbf{F}^\top$ and $\mathbf{X} := 2\mathbf{F}\,\mathrm{diag}(\mathbf{x})\mathbf{F}^\top$, see also [9] for a similar derivation. As evidenced by (8) and different from transmission grids, voltage magnitudes in distribution grids depend not only on reactive, but on active injections as well. Model (8) shows that the dependence is roughly linear.

## III. Voltage Regulation Schemes

Regulating voltage $\mathbf{v}$ by controlling $\mathbf{q}$ through the reactive power capabilities of DGs can be posed as

$$\min_{\mathbf{q}\in\mathcal{Q}} f(\mathbf{q}) + c(\mathbf{q}) \tag{9}$$

where $f(\mathbf{q})$ is the cost of squared voltage magnitudes in $\mathbf{v}$ deviating from their nominal value $v_0\mathbf{1}$; $c(\mathbf{q})$ models the potential cost for reactive power compensation; and $\mathcal{Q}$ is the feasible set of reactive injections. These three components are elaborated next.

Starting with the feasible set $\mathcal{Q}$, DG units have limited reactive power resources. The PV power inverter found on bus $n$ has limited apparent power capability $s_n$. Thus, reactive injections $\mathbf{q}$ should satisfy the box constraints

$$\mathcal{Q} := \{\mathbf{q} : -\bar{\mathbf{q}} \leq \mathbf{q} \leq \bar{\mathbf{q}}\} \tag{10}$$

with $\bar{\mathbf{q}} := [\sqrt{s_1^2 - p_1^2} \ \ldots \ \sqrt{s_N^2 - p_N^2}]^\top$.

A meaningful choice for function $f(\mathbf{q})$ in (9) would be the Euclidean distance between squared voltage magnitudes and their nominal value, that is $\|\mathbf{v} - v_0\mathbf{1}\|_2^2$. Unfortunately, such a choice is not amenable to localized solutions. Then, a reasonable alternative for $f(\mathbf{q})$ would be to minimize the sum of the squared voltage *differences* between every bus and its parent bus. Such a criterion is meaningful, since the grid is connected and the substation voltage is fixed at $v_0$. As originally shown in [9], in order to arrive at localized updates, the squared differences are actually normalized by $x_n$. If $\tilde{\mathbf{v}} = [v_0 \ \mathbf{v}^\top]^\top$, the vector $\tilde{\mathbf{A}}\tilde{\mathbf{v}}$ provides the voltage differences between buses and their parent buses. These differences can be alternatively expressed as

$$\tilde{\mathbf{A}}\tilde{\mathbf{v}} = \mathbf{A}\mathbf{v} + \mathbf{a}_0 v_0 = \mathbf{A}(\mathbf{v} - v_0\mathbf{1})$$

and the voltage deviation cost can be defined as

$$\begin{aligned} f(\mathbf{q}) &:= \frac{1}{4}\sum_{n=1}^{N} \frac{(v_{\pi_n} - v_n)^2}{x_n} \\ &= \frac{1}{4}\|\operatorname{diag}^{-1/2}(\mathbf{x})\mathbf{A}[\mathbf{v}(\mathbf{q}) - v_0\mathbf{1}]\|_2^2 \\ &= \frac{1}{2}\|\mathbf{X}^{-1/2}[\mathbf{v}(\mathbf{q}) - v_0\mathbf{1}]\|_2^2 \\ &= \frac{1}{2}\|\mathbf{X}^{-1/2}(\mathbf{R}\mathbf{p} + \mathbf{X}\mathbf{q})\|_2^2. \end{aligned} \tag{11}$$

The voltage deviation cost of (11) has been reported in [9] by reverse engineering the IEEE 1547.8 standard [14]. The critical property for this choice of voltage deviation cost is that its gradient is simply the deviation of squared voltage magnitudes from the nominal namely [cf. (11)]

$$\nabla f(\mathbf{q}^t) = \mathbf{R}\mathbf{p} + \mathbf{X}\mathbf{q}^t = \mathbf{v}(\mathbf{q}^t) - v_0\mathbf{1} \tag{12}$$

whose $n$-th entry can be measured locally at every bus $n$. It is assumed here that loads follow a constant-power model; therefore, voltage magnitude fluctuations do not automatically alter power injections.

Concerning the reactive power compensation cost $c(\mathbf{q})$, it is typically separable over buses, i.e., $c(\mathbf{q}) = \sum_{n=1}^{N} c_n(q_n)$.

**Algorithm 1** Proximal Gradient for Voltage Regulation

**Input:** Step size $\mu \in (0, 2/\lambda_{\max}(\mathbf{X}))$.

1: Initialize $\mathbf{q}^0 = \mathbf{0}$
2: **for** $t = 1, 2, \ldots$ and at every bus $n$ **do**
3: Locally measure $y_n^t = q_n^t - \mu(v_n^t - v_0)$.
4: Update $q_n^{t+1} = \operatorname{prox}_{c,\mathcal{Q}}^{\mu}[y_n^t]$ based on (19).
5: **end for**

Since negative and positive reactive power injections are equally important, a reasonable option could be

$$c(\mathbf{q}) = \sum_{n=1}^{N} c_n|q_n| \tag{13}$$

where $c_n$ is the marginal reactive support cost for DG unit $n$.

### A. Voltage Regulation via Proximal Gradient

Putting pieces together, the proposed approach to voltage regulation would result by solving the problem [cf. (9)–(13)]

$$\begin{aligned} \min_{\mathbf{q}} \quad & \frac{1}{2}\|\mathbf{X}^{-1/2}(\mathbf{R}\mathbf{p} + \mathbf{X}\mathbf{q})\|_2^2 + \sum_{n=1}^{N} c_n|q_n| \\ \text{s.to} \quad & -\bar{\mathbf{q}} \leq \mathbf{q} \leq \bar{\mathbf{q}}. \end{aligned} \tag{14}$$

Since the objective in (14) is the sum of a differentiable convex function and a non-differentiable one, the problem can be solved via a proximal gradient scheme [18]. Specifically, reactive power injections can be iteratively updated as

$$\mathbf{q}^{t+1} = \operatorname{prox}_{c,\mathcal{Q}}^{\mu}[\mathbf{q}^t - \mu\nabla f(\mathbf{q}^t)] \tag{15}$$

for an appropriately selected step size $\mu > 0$. Expanding the proximal operator yields the equivalent formulation

$$\begin{aligned} \mathbf{q}^{t+1} := \arg\min_{\mathbf{q}} \quad & \sum_{n=1}^{N} c_n|q_n| + \frac{1}{2\mu}\|\mathbf{q} - \mathbf{q}^t + \mu\nabla f(\mathbf{q}^t)\|_2^2 \\ \text{s.to} \quad & -\bar{\mathbf{q}} \leq \mathbf{q} \leq \bar{\mathbf{q}}. \end{aligned} \tag{16}$$

The optimization in (16) is separable across buses. In particular, if bus $n$ computes locally the quantity

$$y_n^t := q_n^t - \mu(v_n^t - v_0) \tag{17}$$

then solving problem (16) amounts to solving in parallel the ensuing problems for all $n \in \mathcal{N}$

$$q_n^{t+1} = \arg\min_{-\bar{q}_n \leq q_n \leq \bar{q}_n} \ c_n|q_n| + \frac{1}{2\mu}\left(q_n - y_n^t\right)^2. \tag{18}$$

The minimizer of (18) yields the local control rule (see [15, Prop. 1] for a proof):

$$q_n^{t+1} = \begin{cases} \bar{q}_n & , \ y_n^t > \bar{q}_n + \mu c_n \\ y_n^t - \mu c_n & , \ \mu c_n < y_n^t \leq \bar{q}_n + \mu c_n \\ 0 & , \ -\mu c_n \leq y_n^t \leq \mu c_n \\ y_n^t + \mu c_n & , \ -\bar{q}_n - \mu c_n \leq y_n^t < -\mu c_n \\ -\bar{q}_n & , \ y_n^t < -\bar{q}_n - \mu c_n \end{cases}. \tag{19}$$

Hence, it has been shown that the proximal gradient algorithm tabulated as Algorithm 1 solves the voltage regulation problem in (14).

**Algorithm 2** Accelerated Voltage Regulation Scheme

**Input:** Step size $\mu \in (0, 2/\lambda_{\max}(\mathbf{X}))$.

1: Initialize $\mathbf{q}^0 = \mathbf{0}$
2: **for** $t = 1, 2, \ldots, 2\sqrt{\kappa(\mathbf{X})}$, and at every bus $n$ **do**
3: Locally measure $y_n^t = q_n^t - \mu(v_n^t - v_0)$.
4: Update $\gamma_t$ and $\theta_t$ from (20)–(21).
5: Extrapolate as $\tilde{y}_n^t = (1 + \gamma_t)y_n^t - \gamma_t y_n^{t-1}$.
6: Update $q_n^{t+1} = \text{prox}_{c,\mathcal{Q}}^{\mu}[\tilde{y}_n^t]$ based on (19).
7: **end for**

The proximal gradient scheme of (19) converges to the minimizer of (14) when the step size $\mu$ lies in $(0, 2/\lambda_{\max}(\mathbf{X}))$; see e.g., [18]. If $\mu = \lambda_{\max}^{-1}(\mathbf{X})$, the convergence of (19) is linear. The latter means that an $\epsilon$-optimal cost value can be attained within $-\frac{2\log\epsilon}{\log 2}\kappa(\mathbf{X})$ iterations, where $\kappa(\mathbf{X}) := \lambda_{\max}(\mathbf{X})/\lambda_{\min}(\mathbf{X})$ is the condition number of $\mathbf{X}$. Given that actual distribution grids can exhibit relatively large $\kappa(\mathbf{X})$ (cf. Section IV for examples), schemes with faster convergence are highly desirable.

### *B. Accelerated Voltage Regulation*

To improve the convergence rate of Algorithm 1, Nesterov's accelerated method [17] is adapted to the present context. Define first the sequence

$$\gamma_t = \frac{\theta_{t-1} - 1}{\theta_t}, \ t \geq 1 \tag{20}$$

where $\theta_t$ is recursively defined as

$$\theta_t = \frac{1}{2}\left(1 + \sqrt{1 + 4\theta_{t-1}^2}\right) \tag{21}$$

and it is initialized at $\theta_{-1} = 0$.

Based on sequence $\gamma_t$, standard proximal gradient iterations can be modified as follows. At iteration $t$, an intermediate point $\tilde{\mathbf{q}}$ is constructed by extrapolating the two most recent values of the original variable, that is

$$\tilde{\mathbf{q}}^t := (1 + \gamma_t)\mathbf{q}^t - \gamma_t \mathbf{q}^{t-1}. \tag{22}$$

It is worth mentioning that albeit both $\mathbf{q}^t$ and $\mathbf{q}^{t-1}$ belong to $\mathcal{Q}$, the auxiliary point $\tilde{\mathbf{q}}^t$ may not.

The accelerated scheme performs a proximal gradient step not on the original variable $\mathbf{q}^t$, but rather on the intermediate point $\tilde{\mathbf{q}}^t$, that is

$$\mathbf{q}^{t+1} := \text{prox}_{c,\mathcal{Q}}^{\mu}[\tilde{\mathbf{q}}^t - \mu\nabla f(\tilde{\mathbf{q}}^t)]. \tag{23}$$

To implement (23), we only need to measure the entries of $\nabla f(\tilde{\mathbf{q}}^t)$ at every bus since $\tilde{\mathbf{q}}^t$ is readily available. Using (12), one can apply $\tilde{\mathbf{q}}^t$ to the distribution grid and then measure the incurred voltage deviations $\mathbf{v}(\tilde{\mathbf{q}}^t) - v_0\mathbf{1}$. Such an approach faces two challenges. It first doubles the number of control actions on the grid by applying both $\mathbf{q}_t$ and $\tilde{\mathbf{q}}_t$. It is further impractical since the reactive injection vector $\tilde{\mathbf{q}}^t$ may be infeasible.

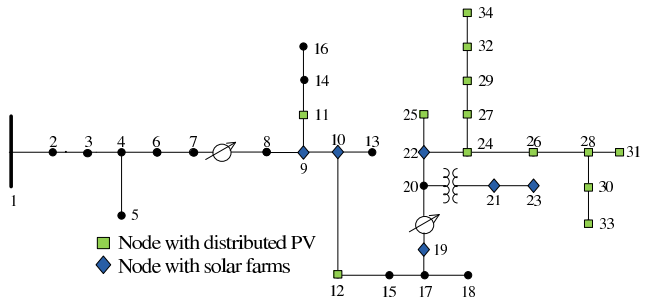


Fig. 2. IEEE 34-bus feeder.

Fortunately, the linearity of $\nabla f$ allows us to evaluate the gradient at the intermediate point $\nabla f(\tilde{\mathbf{q}}^t)$ in a practically feasible way as

$$\begin{aligned}\nabla f(\tilde{\mathbf{q}}^t) &= (1 + \gamma_t)\nabla f(\mathbf{q}^t) - \gamma_t \nabla f(\mathbf{q}^{t-1}) \\ &= (1 + \gamma_t)(\mathbf{v}^t - v_0\mathbf{1}) - \gamma_t(\mathbf{v}^{t-1} - v_0\mathbf{1}).\end{aligned} \tag{24}$$

Equation (24) suggests that the gradient of $f(\mathbf{q})$ can be evaluated at the intermediate point $\tilde{\mathbf{q}}^t$ via an extrapolation step between the two most recent voltage deviation measurements.

The modified voltage regulation scheme is listed as Alg. 2. Its convergence is guaranteed for $\mu \in (0, 1/\lambda_{\max}(\mathbf{X}))$ [17]. Moreover, if $\mu = \lambda_{\max}^{-1}(\mathbf{X})$ and the sequences $\{\theta_t, \gamma_t\}$ are reset every $2\sqrt{\kappa(\mathbf{X})}$ iterations, then an $\epsilon$-optimal cost value can be attained after $-\frac{2\log\epsilon}{\log 2}\sqrt{\kappa(\mathbf{X})}$ iterations. For grids with high condition numbers, the proposed voltage regulation scheme offers significantly accelerated convergence as verified in the next section.

## IV. Numerical Tests

The novel voltage regulation schemes are evaluated using the IEEE 13-bus and 34-bus feeders (shown in Figure 2) [23]. The original multiphase grids are converted to single-phase ones via the procedure described in [10]: All buses are assumed to be served by all three phases, and loads are averaged over the phases. Mutual phase impedances are ignored, and the diagonal entries of the bus impedance matrix are substituted by their mean. Thus, a three-phase grid decouples to three identical single-phase grids. Distributed load is modeled as two identical spot loads at each end of the line. Closed switches are modeled as distribution lines of the same conductor type and length as its direct descendant with the smallest number. Tranformer tap ratios are fixed. To realistically simulate renewables, real PV solar data were obtained from the Smart* project [4]. Solar generation data from 13:00 EDT on August 24, 2011, and from three panels were normalized to unity.

The first experiment uses the 13-bus feeder with condition number $\kappa(\mathbf{X}) = 716$. Loads are set to 80% of their peak value. Solar generation is installed on buses 2, 3, 5-7, 10, 11 and 13; while 52% PV penetration, defined as peak PV power to peak load apparent power, is assumed. Marginal reactive support costs $c_n$ are set to 0.0125 ¢/kVar& h for all $n$.

To serve as a benchmark, the optimization problem in (14) is solved centrally using MATLAB, and the optimal cost value

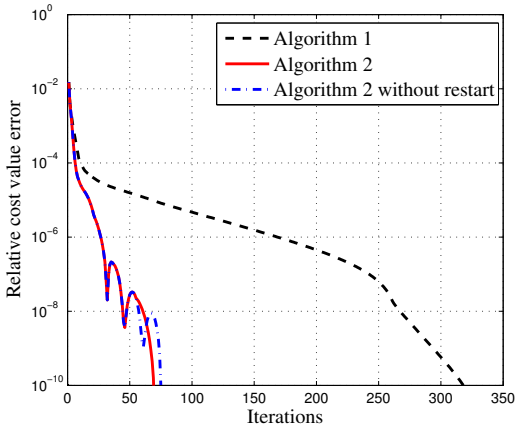


Fig. 3. Convergence performance in the IEEE 13-bus feeder with the optimal step size ($\mu = 1/\lambda_{\max}(\mathbf{X})$).

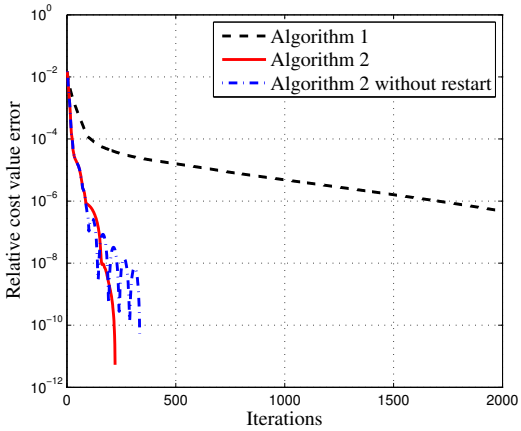


Fig. 4. Convergence performance in the IEEE 13-bus feeder with the suboptimal step size ($\mu = 0.1/\lambda_{\max}(\mathbf{X})$).

is thus obtained. The relative cost value error attained by the proposed schemes for $\mu = 1/\lambda_{\max}(\mathbf{X})$ is shown in Fig. 3. The curves clearly demonstrate that Alg. 2 converges much faster even without resetting sequences $(\gamma_t, \theta_t)$.

Due to the occasional reconfiguration of distribution grids, $\lambda_{\max}(\mathbf{X})$ may not be precisely known. In this case, the step size should be conservatively set to a smaller value to guarantee convergence. Figure 4 depicts the performance of the two algorithms for $\mu = 0.1/\lambda_{\max}(\mathbf{X})$. The plots indicate that the speedup advantage of Algorithm 2 is robust to the choice of step size.

To evaluate accuracy of the linearized grid model, the two algorithms were also tested using the full AC model. In this case, actual nodal voltage magnitudes were obtained using the forward-backward sweep algorithm [16]. The squared voltage magnitudes obtained under the two control rules for both the approximate linearized and the full AC model, are shown in Fig. 5. The curves indicate superior convergence of the accelerated algorithm. They further suggest that the linearized model offers a good approximation.

The second experiment involves the 34-bus feeder shown in Fig. 2 having condition number $5.5 \times 10^4$. A 50% PV penetration level has been assumed on the buses 11, 12, and 24-34. In addition, 6 solar farms are located on buses 9, 10, 19, and 21-23. The solar capacity for the first two farms is 0.15 MVA and for the rest is 0.2 MVA, while they are all assumed to generate 45% of their capacity. The step size is conservatively set to $\mu = 0.1/\lambda_{\max}(\mathbf{X})$. The curves for Alg. 2 with and without resetting coincide because the algorithm converges very fast. Figure 6 corroborates the superior convergence of Alg. 2 over Alg. 1.

Checking the accuracy of the linearized model in (8), the initial condition for DG reactive power injections was also tested using the full AC model for the two systems. The maximum error in the voltage magnitudes over all buses and the corresponding relative error are listed in Table I.

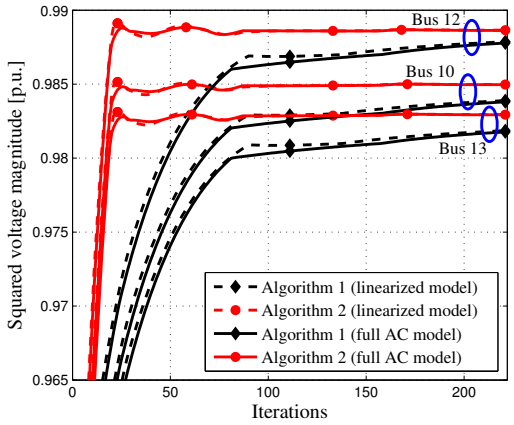


Fig. 5. Voltage profiles of buses 10, 12 and 13 in the IEEE 13-bus feeder.

## V. Conclusions

Voltage regulation schemes for single-phase distribution grids have been considered in this work. Considering limited reactive power resources, a reactive compensation cost, and a rotated voltage deviation penalty, a control rule suggested by the IEEE 1547 standard was implemented as a proximal gradient algorithm. Interpreted as such, its speed of convergence was shown to be bounded by the grid topology. Upon applying Nesterov's acceleration method, a novel localized control rule was developed. The latter converges to the same voltage regulation cost within one fourth of the time needed by the original rule. Therefore, a minor modification in the reactive control rule implemented by DGs offers faster regulation of voltage magnitude profiles. Extensions to unbalanced grids is an interesting research direction.

## Appendix

*Proof of Proposition 1:* Claim *(a)* follows directly from the nullspace property $\tilde{\mathbf{A}}\mathbf{1}_{N+1} = \mathbf{0}$ and the invertibility of $\mathbf{A}$.

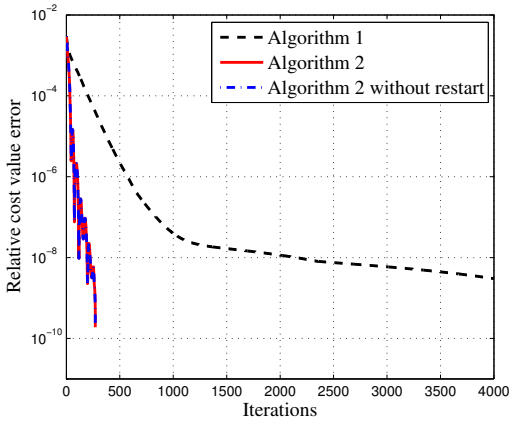


Fig. 6. Convergence performance of algorithms for the 34-bus feeder.

TABLE I
ACCURACY OF LINEARIZED POWER FLOW

| Feeders | error v [p.u.] | relative error [%] |
|---|---|---|
| IEEE 13-bus | $1.3 \times 10^{-3}$ | $1.4 \times 10^{-1}$ |
| IEEE 34-bus | $8.4 \times 10^{-4}$ | $8.7 \times 10^{-2}$ |

For claim (b), consider the $n$-th row of $-\mathbf{A}$ related to line $n$ between buses $(\pi_n, n)$. By definition, $\mathbf{A}_{n,\pi_n} = 1$, $\mathbf{A}_{n,n} = -1$, and the remaining entries of row $n$ are zero. Since $\pi_n < n$, matrix $\mathbf{A}$ is lower triangular, and as such, its negative inverse is lower triangular too.

Concerning (c), $-\mathbf{A}$ has unity eigenvalues because it is lower triangular with all ones on the diagonal. Its inverse $\mathbf{F}$ has obviously unity eigenvalues as well.

For claim (d), $-\mathbf{A}$ is an M-matrix because it has non-positive off-diagonal entries and positive (unity) eigenvalues [13, Sec. 2.1]. It follows that its inverse is non-negative.

For claim (e), note first that $\mathbf{F}$ has all ones on the diagonal due to claim (c). From $-\mathbf{AF} = \mathbf{I}$, the $n$-th column of $\mathbf{F}$ denoted by $\mathbf{f}_n$ should satisfy $-\mathbf{A}\mathbf{f}_n = \mathbf{e}_n$. The first $n$ equations of $-\mathbf{A}\mathbf{f}_n = \mathbf{e}_n$ are trivially satisfied; the remaining ones yield $\sum_{k=1}^{N} \mathbf{A}_{m,k}\mathbf{F}_{k,n} = 0$ for $m = n+1, \ldots, N$. Since the only non-zero entries of the $m$-th row of $\mathbf{A}$ are $\mathbf{A}_{m,\pi_m} = 1$ and $\mathbf{A}_{m,m} = -1$, the last equations yield

$$\sum_{k=1}^{N} \mathbf{A}_{m,k}\mathbf{F}_{k,n} = \mathbf{A}_{m,\pi_m}\mathbf{F}_{\pi_m,n} - \mathbf{F}_{m,n} = 0 \qquad (25)$$

for $m = n+1, \ldots, N$. Three cases can be identified.

**(c1)** If $\pi_m < n$, equation (25) implies $\mathbf{F}_{m,n} = 0$ since $\mathbf{F}_{\pi_m,n} = 0$ since $\mathbf{F}$is lower triangular.

**(c2)** If $\pi_m = n$, equation (25) yields $\mathbf{F}_{m,n} = 1$ because $\mathbf{A}_{m,\pi_m} = \mathbf{F}_{n,n} = 1$.

**(c3)** If $\pi_m > n$, it follows that $\mathbf{F}_{m,n} = \mathbf{F}_{\pi_m,n}$. The recursion $\mathbf{F}_{m,n} = \mathbf{F}_{\pi_m,n} = \mathbf{F}_{\pi_{\pi_m},n} = \ldots$ can be terminated either in (c2) yielding $\mathbf{F}_{m,n} = 1$ if $m \in \mathcal{D}_n$, or in (c1) if $m \notin \mathcal{D}_n$ yielding $\mathbf{F}_{m,n} = 0$, thus proving claim (e). ■

## REFERENCES


[1] "Facts on California solar industry," Solar Energy Industry Association, Tech. Rep., 2014. [Online]. Available: http://www.seia.org/state-solar-policy/california

[2] M. Baran and I. El-Markabi, "A multiagent-based dispatching scheme for distributed generators for voltage support on distribution feeders," *IEEE Trans. Power Syst.*, vol. 22, no. 1, pp. 52–59, Feb. 2007.

[3] M. Baran and F. Wu, "Optimal capacitor placement on radial distribution systems," *IEEE Trans. Power Syst.*, vol. 4, no. 1, pp. 725–734, Jan. 1989.

[4] S. Barker, A. Mishra, D. Irwin, E. Cecchet, P. Shenoy, and J. Albrecht, "Smart*: An open data set and tools for enabling research in sustainable homes," in *Workshop on Data Mining Applications in Sustainability*, Beijing, China, Aug. 2012.

[5] M. Bazrafshan and N. Gatsis, "Decentralized stochastic programming for real and reactive power management in distribution systems," in *Proc. IEEE Intl. Conf. on Smart Grid Commun.*, Venice, Italy, Nov. 2014, pp. 218–223.

[6] S. Bolognani, R. Carli, G. Cavraro, and S. Zampieri, "A distributed control strategy for optimal reactive power flow with power constraints," in *Proc. IEEE Conf. on Decision and Control*, Florence, Italy, Dec. 2013.

[7] S. Deshmukh, B. Natarajan, and A. Pahwa, "Voltage/VAR control in distribution networks via reactive power injection through distributed generators," *IEEE Trans. Smart Grid*, vol. 3, no. 3, pp. 1226–1234, Sep. 2012.

[8] M. Farivar, R. Neal, C. Clarke, and S. Low, "Optimal inverter VAR control in distribution systems with high PV penetration," in *Proc. IEEE Power & Energy Society General Meeting*, San Diego, CA, Jul. 2012.

[9] M. Farivar, L. Chen, and S. Low, "Equilibrium and dynamics of local voltage control in distribution systems," in *Proc. IEEE Conf. on Decision and Control*, Florence, Italy, Dec. 2013, pp. 4329–4334.

[10] L. Gan, N. Li, U. Topcu, and S. Low, "On the exactness of convex relaxation for optimal power flow in tree networks," in *Proc. IEEE Conf. on Decision and Control*, Maui, HI, Dec. 2012, pp. 465–471.

[11] B. Gentile, J. Simpson-Porco, F. Dorfler, S. Zampieri, and F. Bullo, "On reactive power flow and voltage stability in microgrids," in *Proc. American Control Conference*, Portland, OR, Jun. 2014, pp. 759–764.

[12] G. B. Giannakis, V. Kekatos, N. Gatsis, S.-J. Kim, H. Zhu, and B. Wollenberg, "Monitoring and optimization for power grids: A signal processing perspective," *IEEE Signal Processing Mag.*, vol. 30, no. 5, pp. 107–128, Sep. 2013.

[13] R. A. Horn and C. R. Johnson, *Topics in Matrix Analysis*. Cambridge University Press, 1991.

[14] *IEEE 1547 Standard for Interconnecting Distributed Resources with Electric Power Systems*, IEEE Std., 2014. [Online]. Available: http://grouper.ieee.org/groups/scc21/1547/1547_index.html

[15] V. Kekatos, G. Wang, A. J. Conejo, and G. B. Giannakis, "Stochastic reactive power management in microgrids with renewables," *IEEE Trans. Power Syst.*, 2015, early access.

[16] W. H. Kersting, *Distribution System Modeling and Analysis*. Boca Raton, FL: CRC Press, 2002.

[17] Y. Nesterov, *Introductory Lectures on Convex Optimization*. Boston, MA: Kluwer, 2004.

[18] N. Parikh and S. Boyd, "Proximal algorithms," *Foundations and Trends in Optimization*, vol. 1, no. 3, pp. 127–239, 2014.

[19] Q. Peng and S. Low, "Distributed algorithm for optimal power flow on a radial network," in *Proc. IEEE Conf. on Decision and Control*, Venice, Italy, Dec. 2014, pp. 167–172.

[20] B. Robbins, C. Hadjicostis, and A. Dominguez-Garcia, "A two-stage distributed architecture for voltage control in power distribution systems," *IEEE Trans. Power Syst.*, vol. 28, no. 2, pp. 1470–1482, May 2013.

[21] P. Sulc, S. Backhaus, and M. Chertkov, "Optimal distributed control of reactive power via the alternating direction method of multipliers," *IEEE Trans. Energy Conversion*, vol. 29, no. 4, pp. 968–977, Dec. 2014.

[22] K. Turitsyn, P. Sulc, S. Backhaus, and M. Chertkov, "Options for control of reactive power by distributed photovoltaic generators," *Proc. IEEE*, vol. 99, no. 6, pp. 1063–1073, Jun. 2011.

[23] Power systems test case archive. Univ. of Washington. [Online]. Available: http://www.ee.washington.edu/research/pstca/

[24] B. Zhang, A. Dominguez-Garcia, and D. Tse, "A local control approach to voltage regulation in distribution networks," in *Proc. North American Power Symposium*, Manhattan, KS, Sep. 2013.